B. Cotterell
Institute of Materials Research and Engineering,
Singapore 117602

Z. Chen
School of Materials Engineering,
Nanyang Technological University,
Singapore 639798

J.-B. Han

N.-X. Tan

Agilent Technologies Singapore Pte. Ltd.,
Singapore 618494

The Strength of the Silicon Die in Flip-Chip Assemblies

The mechanical reliability of silicon dies is affected by the defects introduced by surface grinding and edge dicing. The ring-on-ring and the four-point-bend test have been used in this study to separate the distribution in strength for these two types of defect. At low probabilities of failure, it is the "strength" of the edge defects that dominate the reliability. However, if the edges of the die are only lightly stressed compared with the surface, edge defects are unlikely to cause fracture. In this case the use of the four-point-bend test, which is sensitive to both edge and surface defects, will result in an underestimate of the reliability and if only one test is to be performed the ring-on-ring test is preferable to the four-point-bend test. Generally, for a full reliability estimate, the distributions of both types of defect need to be determined. [DOI: 10.1115/1.1535934]

Keywords: *Strength, Reliability, Silicon, Grinding Defects, Dicing Defects*

Introduction

Underfill is used in flip chips with organic substrates to reduce the shear on the solder balls and consequent fatigue under thermal cycling. The substrate is mechanically linked to the die and the thermal mismatch causes bending of the silicon die. The demand for larger die sizes leads to higher stresses, which may cause die cracking [1]. As far as mechanical reliability is concerned only surface or edge defects are significant. Die cracks can initiate at surface grinding defects in the tension backside of the die at edge dicing defects [1,2] or at divots produced by the pins, which separate the backside of the die from the film-mounted diced wafer [3]. In this paper only grinding and dicing defects are considered. Cracks from surface defects propagate from the backside of the die towards the printed circuit board under the action of the bending stress (see Fig. 1(*a*)). As these cracks approach the opposite compression face of the die they may turn to propagate along the die. The edge of the die is virtually free from bending stresses but a transverse tensile stress, enhanced by the corner of the fillet to the underfill, can cause the initiation of a crack, which is likely to turn, after propagating a short distance, towards the backside of the die [1] as shown in Fig. 1(*b*).

The cleavage planes with the lowest fracture toughness in silicon are the {111} planes where $K_{Ic}=0.82\ \text{MPA}\sqrt{\text{m}}$, but the fracture toughness is not that much greater on the {001} planes where $K_{Ic}=0.90\ \text{MPa}\sqrt{\text{m}}$ [4]. The surfaces of silicon wafers are {001} planes so that cracking from its surface is most likely if the maximum stress is in a ⟨110⟩ direction. The stress acting across a {111} is at most half the in-plane stress. Hence it is not surprising that fractures initiated on a free {001} surface stressed in a ⟨110⟩ direction initially propagate on a {110} plane normal to the {001} surface and only kink out of that plane into a {111} surface after propagating some distance into the specimen [4].

Die cracking depends upon both the stress and the size of the defect. There is no one value that can be assigned to the strength of the die but only a probability of fracture which relates to the chance of finding a critical defect at any stress level. The statistics of fracture of brittle materials was first established by [5]; more recently it has been reinterpreted in terms of fracture mechanics and flaw sizes [6], but in practice one can still talk of a "strength" of a flaw or defect. A favorite test geometry to determine the "strength" distribution of defects is the four-point-bend (see Fig. 2). However, in the usual Weibull analysis no distinction is made between the type of defects present in this geometry. The mechanical reliability of a silicon die in a flip-chip assembly depends upon both the surface defects due to the grinding of the wafer and the edge defects introduced by dicing the wafer into the dies. Here both the "strength" distribution of the surface and edge defects are considered and a method of separating the distributions of the surface grinding and edge dicing defects by performing two series of tests presented. With this knowledge the effect of the grinding and dicing machining parameters on reliability can be determined. The two tests chosen are the ring-on-ring test (see Fig. 3) which is a quasi axisymmetric equivalent of the four-point-bend test in which there are no stressed edges so that the strength is determined by the surface defects alone, and the four-point-bend test whose strength is determined by both edge and surface defects. The strategy is to find the probability "strength" distribution of the surface flaws from the ring-on-ring test and then to analyze the strength distribution of the four-point-bend test using the "strength" distribution of the surface flaws to enable the probability "strength" distribution of the edge flaws to be separated from the total strength distribution.

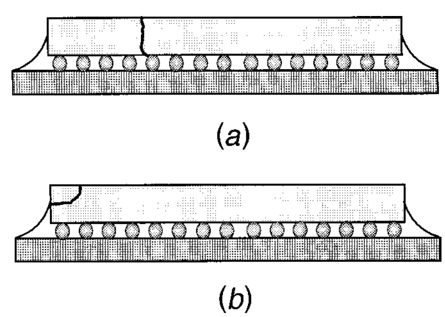

Fig. 1 Silicon die cracks in flip chip assemblies—(*a*) cracks from surface defects, (*b*) cracks from edge defects

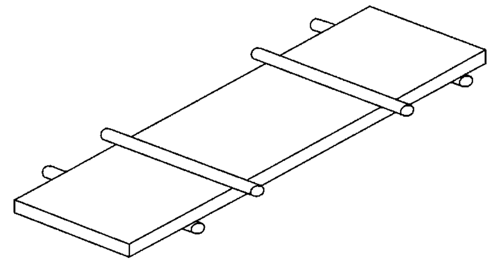

Fig. 2 The four-point-bend test

Contributed by the Electronic and Photonic Packaging Division for publication in the JOURNAL OF ELECTRONIC PACKAGING. Manuscript received by the EPPD Division, December 27, 2001, Associate Editor: K. Kishimoto.

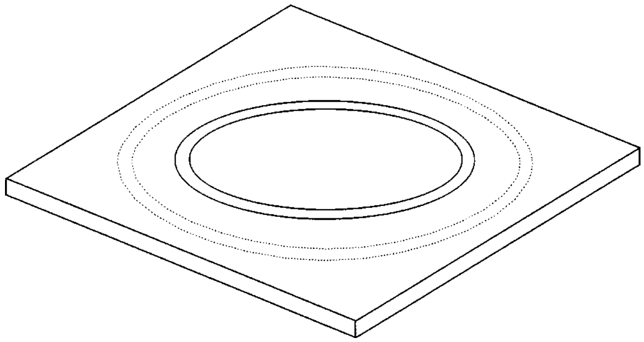

Fig. 3 The ring-on-ring test

Weibull Strength Distribution

Using an exponential distribution for the risk of rupture, Weibull [5] derived a probability of fracture, $P(V)$, given by

$$P(V)=1-\exp-\int_V(\sigma/\sigma_0)^m\rho dV \quad (1)$$

where m is the Weibull modulus, σ_0 is a reference stress, ρ is the density of the defects, and V is the volume, area, or length depending on the whether the significant defects are distributed in the body, surface, or edge of the specimen. The Weibull distribution has stood the test of time and is the best available. Only two parameters define the Weibull distribution since it is ρ/σ_0^m that can be determined from strength tests and not ρ and σ_0 separately. In order to simplify the numerical analysis, we normalize the stress by the mean fracture strength, σ_m, of the sample of N specimens given by

$$\sigma_m=\sum_1^N\int_V\sigma\frac{dV}{V} \quad (2)$$

The Weibull strength distribution can then be written as

$$P(V)=1-\exp-\int_V\lambda(\sigma/\sigma_m)^m dV/V \quad (3)$$

where it can be shown that by definition

$$\lambda=\rho V\left(\frac{\sigma_m}{\sigma_0}\right)^m=[\Gamma(1+1/m)]^m \quad (4)$$

Γ being the gamma function. Eq. (3) is the basic equation used in this paper. The mean fracture strength depends upon the size of the specimen since ρ and σ_0 are size independent. Therefore, if σ_{m0} is the mean strength of a reference specimen whose ''volume'' is V_0, then the mean fracture strength, σ_m, for a specimen whose ''volume'' is V is given by

$$\sigma_m=\sigma_{m0}\left(\frac{V_0}{V}\right)^{1/m} \quad (5)$$

This expression predicts the size dependence of the mean stress reasonably accurately if the difference in ''volume'' is small, but becomes inaccurate for very large differences. There are a number of ways of determining the Weibull modulus from experimental results. If the stress is constant, as it is for the four-point-bend geometry[1] or a linear function of load, the probability of fracture, P, is usually obtained from a ranking of the fracture strengths. The probability of fracture is then assumed to be uniformly distributed over the test results. There are various expressions for the probability as a function of the rank. The one that is consistent with the maximum likelihood method described in the forthcoming is that the probability of the ith ranking fracture load, F_i, in a test series of N is given by

$$P_i=\frac{i}{N+1} \quad (6)$$

The Weibull modulus, m, can then be found from the slope of a plot of $\ln(\ln(1/(1\text{-}P))$ versus $\ln(\sigma)$. However, in our case the deflection in the ring-on-ring test is large and the stresses are nonlinear. Also this simple technique cannot be used to separate the effect of surface from edge defects in the four-point-bend test. In this paper the maximum likelihood method is used to determine the Weibull modulus [7]. The method can be most easily appreciated if the stress is constant over the defects. The likelihood, L, of all obtaining the fracture stresses, σ_i, in a test series can be written in terms of the probability density function, $p(\sigma/\sigma_m)$, which is given by

$$p(\sigma/\sigma_m)=\frac{dP}{d(\sigma/\sigma_m)}=\left[m\lambda\int_V\left(\frac{\sigma}{\sigma_m}\right)^{m-1}\frac{dV}{V}\right]\times\left[\exp-\lambda\int_V\left(\frac{\sigma}{\sigma_m}\right)^m\frac{dV}{V}\right] \quad (7)$$

The likelihood of all the fracture strengths occurring, L, is

$$L=p_1p_2\ldots\ldots\ldots\ldots\ldots p_N \quad (8)$$

The best value of m is that which maximizes the likelihood, L.

No matter how many specimens are tested they are only a sample of the population. There is no bias in the mean strength that is the sample mean is the best estimate of the population mean. However, the Weibull modulus, m, of the sample is biased and is always larger than the population modulus m^p [7–10]. Monte Carlo computer experiments, where it is assumed that the population is exactly modeled by a Weibull distribution, have been programmed to calculate the most probable population Weibull modulus, and the standard deviations of that modulus and the mean strength (see Appendix A).

Fracture Tests on Silicon Dies

The inner and outer diameters in the ring test were 9.5 and 19.5 mm, respectively, and for the four-point-bend test the inner and outer spans were 9.6 and 20 mm, respectively. The two sets of specimens for the ring-on-ring and four-point-bend tests were cut from the same batch of commercial silicon wafers, which were 0.481 mm thick. There were 127 specimens in both sets. The specimens were diced, using commercial die dicing equipment, with their sides on {110} planes. The set used in the ring-on-ring tests was 25 mm square and the width for four-point-bend test, 7.37 mm, was chosen so that the test areas in both sets were the same and no correction for specimen size need be made. The protective plastic was removed and attached to the compressive passivation side to enable the fracture fragments to be preserved. This procedure does not affect the fracture process.

Since the placement of the square specimens used in the ring-on-ring tests affects the stress distribution, a template was used to ensure accurate alignment. Both sets of specimen were tested in an Instron 5543 testing machine with a crosshead speed of 0.2 mm/min at ambient temperature (≈25°C).

Cracks in the ring-on-ring tests formed in the ⟨110⟩ directions parallel to the sides of the specimen. In the four-point-bend tests the cracks formed across the specimens in the ⟨110⟩ direction.

Analysis of the Ring-on-Ring Tests

The deflection was nonlinear because of the membrane stiffness and a finite element analysis was performed which also took account of the orthotropic nature of the silicon (see Appendix B).

[1]The bending stress outside of the inner span in the four-point-bend test decreases linearly to zero at the outside supports. The probability of fracture decreases very much more rapidly, since $m \gg 1$, and the likelihood of fracture outside of the inner span is usually neglected.

Table 1 The Weibull parameters for surface defects in the ring-on-ring test

	m_s		σ_s (MPa)	
	mean	standard deviation	mean	standard deviation
Sample of 127	8.18	-	288	-
Population	8.10	0.56	288	3.8

Table 2 The Weibull parameters for edge defects in the four-point-bend test

	m_e		σ_e (MPa)	
	mean	standard deviation	mean	standard deviation
Sample of 127	3.20	-	314	-
Population	3.19	0.23	314	9.5

The maximum normal surface stresses in the ⟨110⟩ have been expressed by a third order polynomial of the applied load (see Appendix B).

The cracks initiate in the surface so that the integrals are taken over the tensile surface, A, within the inner ring. The mean fracture strength, σ_{ms}, was obtained by numerically integrating the stresses over A and taking the average according to Eq. (2).[2] The probability density function $p(F)$ for fracture at a load F can be written as

$$p(F)=\left[m_s\lambda_s\int_A\left(\frac{\sigma}{\sigma_{ms}}\right)^{m_s-1}\frac{\partial(\sigma/\sigma_{ms})}{\partial F}\frac{dA}{A}\right]\times\left[\exp-\lambda_s\int_A\left(\frac{\sigma}{\sigma_{ms}}\right)^{m_s}\frac{dA}{A}\right] \tag{9}$$

The value of the Weibull modulus that maximizes the likelihood of the experimental results is found numerically. The sample modulus, m_s, and mean strength, σ_{ms} are given in Table 1, which also contains the population values, m_s^p, σ_{ms}^p, and their standard deviations obtained by use of the Monte Carlo method (see Appendix A).

Analysis of the Four-Point-Bend Tests

The membrane stress developed in the four-point-bend test is insignificant, thus the stress is a linear function of the load and can be found from simple bending theory. Since the four-point-bend specimens were obtained from the same batch of wafers as the ring-on-ring specimens, it is assumed that the best estimate of the probability of fracture from surface flaws is given by

$$P_s=1-\exp-\lambda_s^p\left(\frac{\sigma}{\sigma_{ms}^p}\right)^{m_s^p} \tag{10}$$

The probability of fracture from an edge flaw is given by

$$P_e=1-\exp-\lambda_e\left(\frac{\sigma}{\sigma_{me}}\right)^{m_e} \tag{11}$$

Hence the probability of fracture in the four-point-bend test from either a surface or edge defect is given by

$$P=1-\exp-\left[\lambda_{ms}^p\left(\frac{\sigma}{\sigma_{ms}^p}\right)^{m_s^p}+\lambda_e\left(\frac{\sigma}{\sigma_{me}}\right)^{m_e}\right] \tag{12}$$

The probability density function for fracture as a function of the stress normalized by the mean ‘‘strength’’ of both surface and edge defects, σ_m, is given by

$$p\left(\frac{\sigma}{\sigma_m}\right)=\left[\lambda_s^p m_s^p\left(\frac{\sigma}{\sigma_m}\right)^{m_s^p-1}\left(\frac{\sigma_m}{\sigma_{ms}^p}\right)^{m_s^p}+\lambda_e m_e\left(\frac{\sigma}{\sigma_m}\right)^{m_e-1}\left(\frac{\sigma_m}{\sigma_{me}}\right)^{m_e}\right]\times\exp-\left\{\lambda_s^p\left[\left(\frac{\sigma}{\sigma_m}\right)\left(\frac{\sigma_m^p}{\sigma_{ms}^p}\right)\right]^{m_s^p}+\lambda_e\left[\left(\frac{\sigma}{\sigma_m}\right)\left(\frac{\sigma_m}{\sigma_{me}}\right)\right]^{m_e}\right\} \tag{13}$$

[2]The subscript s is used to indicate that fracture initiates from a surface defect and e for a fracture initiating from an edge flaw.

The unknown parameters in Eq. (13) are the Weibull modulus for the edge defects, m_e, and the mean strength of the edge defects, σ_{me}. By definition, the mean of the normalized stress, σ/σ_m, is equal to one. Thus

$$\left(\frac{\sigma}{\sigma_m}\right)_m=\int_0^\infty\left(\frac{\sigma}{\sigma_m}\right)p\left(\frac{\sigma}{\sigma_m}\right)d\left(\frac{\sigma}{\sigma_m}\right)=1 \tag{14}$$

and

$$\int_0^\infty\left(\frac{\sigma}{\sigma_m}\right)p\left(\frac{\sigma}{\sigma_m}\right)d\left(\frac{\sigma}{\sigma_m}\right)=\int_0^\infty\left\{\lambda_s^p m_s^p\left[\left(\frac{\sigma}{\sigma_m}\right)\left(\frac{\sigma_m}{\sigma_{ms}^p}\right)\right]^{m_s^p}+\lambda_e m_e\left[\left(\frac{\sigma}{\sigma_m}\right)\left(\frac{\sigma_m}{\sigma_{me}}\right)\right]^{m_e}\right\}\times\exp-\left\{\lambda_s^p\left[\left(\frac{\sigma}{\sigma_m}\right)\left(\frac{\sigma_m}{\sigma_{ms}^p}\right)\right]^{m_s^p}+\lambda_e\left[\left(\frac{\sigma}{\sigma_m}\right)\left(\frac{\sigma_m}{\sigma_{me}}\right)\right]^{m_e}\right\}d\left(\frac{\sigma}{\sigma_m}\right) \tag{15}$$

The best fit to the experimental results is obtained by maximizing the likelihood given by Eq. (8) with the extra condition given by Eqs. (14) and (15). The values for the Weibull modulus, m_e and the mean ‘‘strength,’’ σ_{me}, of the edge defects are shown in Table 2 together with the population values, m_e^p, σ_{me}^p, and their standard deviations found from computer experiments (see Appendix A).

Discussion of Results

The probability of fracture is not explicitly calculated when the maximum likelihood method is used to evaluate the Weibull modulus. However, to enable the quality of the fit to the experimental method, the probability of fracture obtained by ranking the fracture loads and using Eq. (6) has been calculated. In Fig. 4 the probability of fracture as a function of the fracture strength, normalized by the mean fracture strength, for the ring-on-ring test is

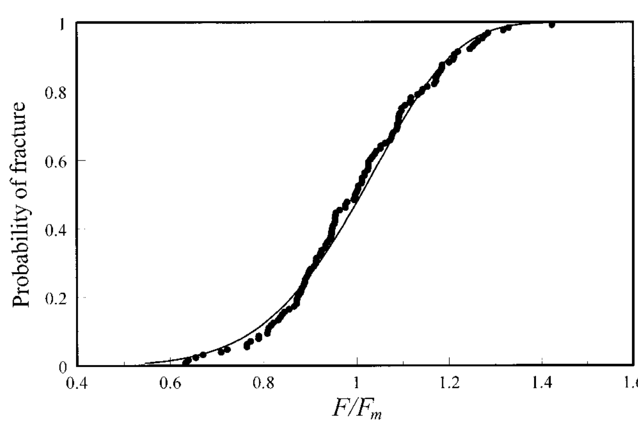

Fig. 4 The probability of fracture from surface defects in the ring-on-ring test

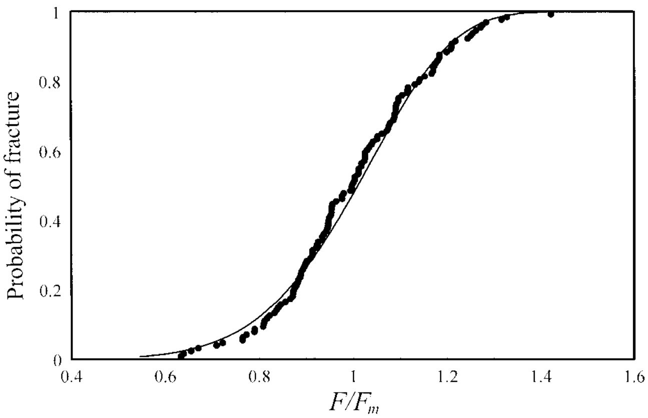

Fig. 5 The probability of fracture in the four-point-bend test

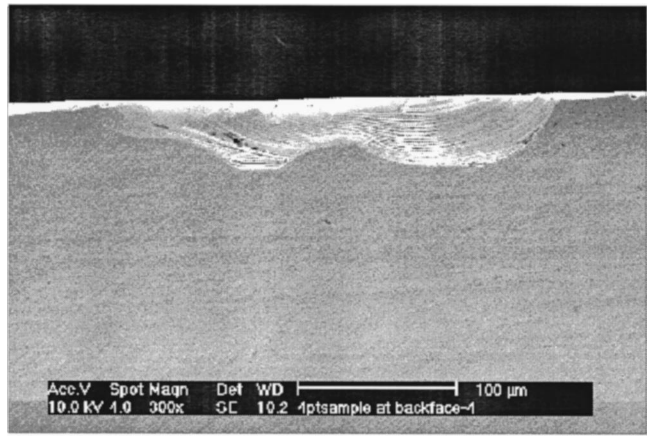

Fig. 7 A large edge defect caused by dicing

compared with the Weibull distribution using the parameters obtained by the method of maximum likelihood. The fit is excellent. The Weibull modulus for the sample of 127 specimens was 8.18. Correcting for the bias in taking samples gives 8.10 as the best estimate of the population Weibull modulus for surface defects. The mean fracture strength is 288 MPa.

Using the population Weibull modulus for service defects with the Weibull modulus of the edge defect as an independent variable with the mean fracture "strength" as a dependent variable, the best estimate has been obtained by the maximum likelihood method from the four-point-bend tests. Using Eq. (12) to estimate the probability of fracture in the four-point-bend test from both surface and edge defects, Fig. 5 has been constructed to allow the goodness of fit with the experiment results, using Eq. 6, to be appreciated. Though the fit is not as good as that for the ring-on-ring test, it is reasonably good giving confidence in the method used to separate the two distributions. Again the population Weibull modulus has been estimated from the value for the sample of 127 specimens. The population Weibull modulus, 3.19, for the edge defects is much smaller, than that for surface defects, and the mean fracture "strength," 314MPa is significantly higher. The population probability of fracture from surface, edge, and combined defects in the four-point-bend test are shown in Fig. 6, the experimental results are also compared with the population probability of fracture in this figure. What is observed is that for low probability of fracture (high reliability), which is the area of interest to the microelectronics industry, it is the edge dicing defects that control the reliability. On the other hand at high probabilities of fracture (low reliability) it is the surface defects that dominate. The low Weibull modulus combined with the high mean fracture "strength" of the edge defects implies that the edge dicing defects are in the form of a few large defects, one such dicing defect is shown in Fig. 7, which occasionally cause very low strength. This conclusion from the statistical analysis is in agreement with SEM observations of the fracture surfaces where it was seen that the low stress fractures initiated at edge defects and the high stress fractures at surface defects.

Although it is fully realised that the silicon die in flip chips is far from uniformly stressed, the probability of fracture of uniformly stressed hypothetical 5 and 20 mm square silicon dies is estimated in Fig. 8. Table 3 shows the effect of size on the mean defect "strengths," which have been calculated using Eq. (5). For a given reliability, the allowable stress is reduced as the size of the silicon die increases. There is little difference in the relative importance of surface and edge defects because, though the area increases as the square of the die size whereas the edge linearly with size, the Weibull modulus for edge defects is much smaller than that for the surface defects and the two effects work against each other.

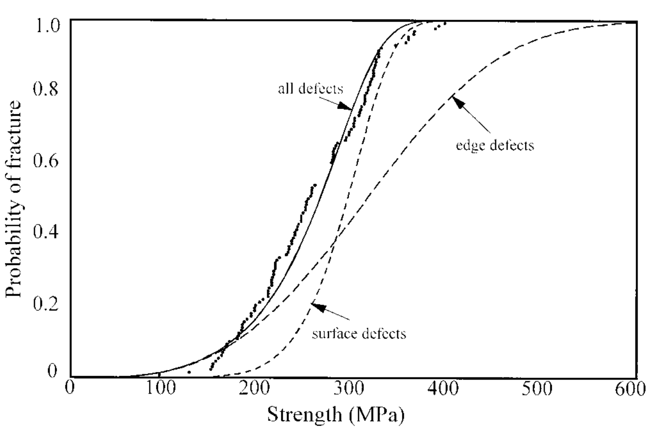

Fig. 6 The best estimates of the population probability of fracture for the four-point-bend test

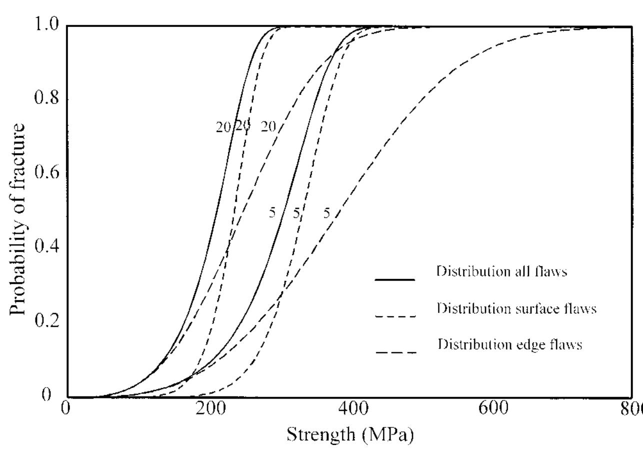

Fig. 8 The size effect on the probability of fracture of a hypothetical uniformly stressed silicon die

Table 3 Size effect on mean strength of hypothetical silicon dies

Die size (mm)	Mean die strength (MPa)	Mean surface strength (MPa)	Mean edge strength (MPa)
20	203	233	250
5	295	327	385

Conclusions

The ring-on-ring test enables the distribution in ''strength'' of surface defects to be determined. In the four-point-bend test fractures can initiate either from a surface or edge defect. A method is presented where the two distributions can be separated if the distribution for surface defects is known.

Surface grinding and edge dicing defects have very different distributions. If the edge of the die in a flip chip is significantly stressed then edge defects must be considered as well as surface ones and control the probability of fracture in the high reliability range. On the other hand, as is more likely, the stresses along the edges of the die in a flip chip assembly are low, and then the four-point bend test alone will not give an accurate assessment of the probability of fracture. In this case the reliability assessed using only the four-point-bend test to estimate the probability of fracture will be very conservative at high levels of reliability. The ring-on-ring test is to be preferred in this case if only a single test is to be used.

For an accurate assessment of the reliability of the die, it is necessary to obtain both the distributions for surface and edge defects from ring-on-ring and four-point-bend tests. The probability of fracture can then be estimated by integrating over both the surface and the edge making full allowance for the effect of size on the mean strengths.

Appendix A: Monte Carlo Computer Experiments to Determine the Population Weibull Modulus and the Standard Deviations

The specimen is assumed to be uniformly stressed with a population probability of fracture given by

$$P=1-\exp-\lambda\left(\frac{\sigma}{\sigma_m^p}\right)^{m^p} \tag{16}$$

The computer program is used to generate results for samples of N tests. The N probabilities of fracture are chosen by generating random numbers between 0 and 1. The normalized fracture stress is calculated from these probabilities. The method of maximum likelihood is then used to calculate the sample Weibull modulus, m, and the mean of the sample σ/σ_m which are different to the population values. This computer experiment is performed 10,000 times and the average and standard deviation of m and σ/σ_m determined. The average value of σ/σ_m is unity, but the average value of m is greater than m^p. However, from the real experiments it is m that is known not m^p. Therefore, the most likely population Weibull modulus has to be found by iteration. For the first run it is assumed that the population Weibull modulus is the experimental one. The expected experimental modulus is then found. The difference between the actual and the expected experimental modulus is then used to correct the assumed population Weibull modulus and the program is run again. This iterative process converges very quickly.

The difference between the population and the best estimate of the sample Weibull modulus for a sample of 127 is only significant if the modulus is small. The population and sample Weibull moduli are given in Tables 1 and 2.

Appendix B: Finite Element Analysis for the Ring-on-Ring Test

In a ring-on-ring test the deflections are large enough to cause the development of significant membrane stress and the stresses are consequently non-linear. The stress inside the inner ring is not exactly uniform for three reasons: the stresses are nonlinear, the outside edge is square, and the silicon is crystalline and orthotropic. A finite element analysis, using ABAQUS, has been used to determine the surface stresses within the inner ring.

The silicon die is oriented with its surface on a {001} crystal plane while the two edges are ⟨110⟩ directions. Due to symmetry,

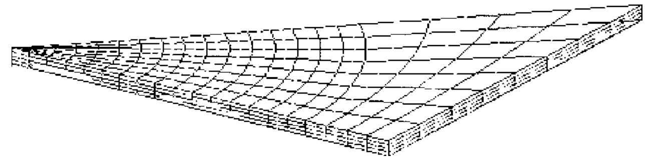

Fig. 9 The finite element mesh

only one-eighth of the square specimen is modeled. Four elements are used through the thickness. Altogether there are 3369 nodes for 640 second-order elements (see Fig. 9). Orthotropic elastic properties of silicon crystal are used in the computation. The stiffness matrix for the stress-strain relationship is [11]

$$\begin{bmatrix}\sigma_{11}\\ \sigma_{22}\\ \sigma_{33}\\ \sigma_{12}\\ \sigma_{13}\\ \sigma_{23}\end{bmatrix}=\begin{bmatrix}194.4 & 35.2 & 194.4 & 0 & 0 & 0\\ 35.2 & 194.4 & 63.9 & 0 & 0 & 0\\ 194.4 & 63.9 & 165.7 & 0 & 0 & 0\\ 0 & 0 & 0 & 50.9 & 0 & 0\\ 0 & 0 & 0 & 0 & 79.6 & 0\\ 0 & 0 & 0 & 0 & 0 & 79.6\end{bmatrix}\begin{bmatrix}\varepsilon_{11}\\ \varepsilon_{22}\\ \varepsilon_{33}\\ \varepsilon_{12}\\ \varepsilon_{13}\\ \varepsilon_{23}\end{bmatrix} \tag{17}$$

where the moduli are in GPa. Subscripts 1 and 2 are along two ⟨110⟩ edges on the {001} surface and direction 3 is along the ⟨100⟩ direction, perpendicular to the surface {001}.

The stresses become more and more nonuniform within the inner ring as the load increases. The maximum of the normal stresses is along the ⟨110⟩ axis under the inner ring and the minimum is at the center. The ratio of the maximum to minimum is no more than 1.08; but when that is raised to a Weibull modulus of 8, it represents a ratio of 1.85 which is quite significant. To validate the FEA the predicted deflection was compared to the experimental deflection.

Because the deflections are large the stresses are a nonlinear function of the applied load, F. To enable the stresses to be incorporated into the statistics program, the maximum normal stress in a ⟨110⟩ direction has been fitted to a third-order polynomial

$$\sigma(r,\theta)=C_1(r,\theta)+C_2(r,\theta)F+C_2(r,\theta)F^2+C_3(r,\theta)F^3 \tag{18}$$

at 17 equally spaced intervals in θ and 17 equally spaced intervals in r along odd numbered radial lines and nine equally spaced intervals along even numbered radial lines (see Fig. 9). A third-order polynomial gives a very good fit (error less than 0.4%) to the finite element results for the range of the experiments.

Nomenclature

C_1, C_2, C_3, C_4 = coefficients for 3rd-order polynomial describing stress
F_i = ith ranking force
i = ranking of strength
K_{Ic} = fracture toughness
m = Weibull modulus
m_e = Weibull modulus for edge defects (sample)
m_e^p = Weibull modulus for edge defects (population)
m_s = Weibull modulus for surface defects (sample)
m_s^p = Weibull modulus for surface defects (population)
N = no. of specimens in sample
P = probability of fracture
P_e = probability of fracture from edge defect
P_i = probability of fracture of ith ranking specimen
P_s = probability of fracture from surface defect
p = probability density function
V = volume, area, or length
V_0 = volume, area, or length of reference specimen
Γ = gamma function
λ = Weibull parameter related to density of defects

References

[1] Ranjan, M., Gopalakrishnan, L., Srihan, K., and Woychik, 1998, ''Die Cracking in Flip Chip Assemblies,'' Proc., 48th Electronic Components and Technology Conference, Seattle, WA, pp. 729–733.

[2] Leung, B., Guo, Y., and Sarihan, V., 1997, ''Die Strength in the Presence of Edge Cracks,'' Application of Fracture Mechanics in Electronic Packaging, eds., W. T. Chen and D. T. Read, ASME, AMD-Vol 222, pp. 125–131.

[3] Popelar, S. F., 1998, ''An Investigation into the Fracture of Silicon Die Used in Flip Chip Applications,'' Proc., Int. Symp. Advanced Packaging Materials, pp. 41–48.

[4] Chen, C. P., and Leipold, M. H., 1980, ''The Fracture Toughness of Silicon,'' Ceram. Bull., **59**, pp. 469–472.

[5] Weibull, W., 1939, *Statistical Theory of Strength of Materials*, Ingeniors Vetenskaps. Akademien, Handkinger No 151.

[6] Jayatilaka, A. De S., and Trustrum, K., 1977, ''Statistical Approach to Brittle Fracture,'' J. Mater. Sci., **12**, pp. 1426–1430.

[7] Trustrum, K., and Jaytilaka, A. De S., 1979, ''On Estimating the Weibull Modulus for a Brittle Material,'' J. Mater. Sci., **14**, pp. 1080–1084.

[8] Bergman, B., 1986, ''Estimation of Weibull Parameters Using a Weight Function,'' J. Mater. Sci. Lett., **5**, pp. 611–614.

[9] Langlois, R., 1991, ''Estimation of Weibull Parameters,'' J. Mater. Sci. Lett., **10**, pp. 1049–1051.

[10] Absi, J., Fournier, P., and Glandis, J. C., 1999, ''Influence of Experimental Parameters on the Estimation of Weibull's Modulus,'' J. Mater. Sci., **34**, pp. 1219–1227.

[11] Mason, W. P., 1958, *Physical Acoustics and the Properties of Solids*, Van Nostrand.